The EMBO Journal Vol. 22 No. 6 pp. 1359–1369, 2003

A novel splicing regulator shares a nuclear import pathway with SR proteins

Ming-Chih Lai[1], Hao-Wei Kuo[1], Wen-Cheng Chang[1,2] and Woan-Yuh Tarn[1,3]

[1]Institute of Biomedical Sciences, Academia Sinica, Taipei and [2]Institute of Anatomy and Cell Biology, National Yang-Ming University, Shih-Pai, Taipei, Taiwan

[3]Corresponding author
e-mail: wtarn@ibms.sinica.edu.tw

Alternative splicing of precursor mRNA is often regulated by serine/arginine-rich proteins (SR proteins) and hnRNPs, and varying their concentration in the nucleus can be a mechanism for controlling splice site selection. To understand the nucleocytoplasmic transport mechanism of splicing regulators is of key importance. SR proteins are delivered to the nucleus by transportin-SRs (TRN-SRs), importin β-like nuclear transporters. Here we identify and characterize a non-SR protein, RNA-binding motif protein 4 (RBM4), as a novel substrate of TRN-SR2. TRN-SR2 interacts specifically with RBM4 in a Ran-sensitive manner. TRN-SR2 indeed mediates the nuclear import of a recombinant protein containing the RBM4 C-terminal domain. This domain serves as a signal for both nuclear import and export, and for nuclear speckle targeting. Finally, both *in vivo* and *in vitro* splicing analyses demonstrate that RBM4 not only modulates alternative pre-mRNA splicing but also acts antagonistically to authentic SR proteins in splice site and exon selection. Thus, a novel splicing regulator with opposite activities to SR proteins shares an identical import pathway with SR proteins to the nucleus.

Keywords: alternative splicing/nuclear import/RNA-binding protein/SR proteins

Introduction

Subcellular compartmentalization of eukaryotic cells necessitates nucleocytoplasmic transport of proteins and other macromolecules across the nuclear envelope (Nakielny and Dreyfuss, 1999). Nuclear transport is an ongoing and constitutive process for a vast number of molecules. It can also be regulated in response to cellular signals or to environmental stimuli, thus providing an additional level of regulation for gene expression in eukaryotes.

Different pathways exist for nucleocytoplasmic transport because of the variety of signals in cargo and their corresponding transport receptors (Mattaj and Englmeier, 1998; Nakielny and Dreyfuss, 1999). Transport signals of proteins show considerable variation in complexity from short peptide motifs to extended domains (Mattaj and Englmeier, 1998; Nakielny and Dreyfuss, 1999). For nuclear import, the nuclear localization signal (NLS) of protein cargo is recognized in the cytoplasm by a heterodimeric transport factor, importin α/β, or directly by importin β or another family member (Nakielny and Dreyfuss, 1999). A complex of import transporter and cargo is subsequently translocated into the nucleus through the channel of the nuclear pore complex (NPC). In the nucleoplasm, high levels of Ran in the GTP-loaded form binds to importin β and thereby triggers cargo release.

Pre-mRNAs are synthesized and subsequently processed in the nucleus of eukaryotic cells. Thus pre-mRNA splicing factors, including small nuclear ribonucleoproteins (snRNPs) and protein factors, are necessarily transported into the nucleus for function. A family of serine/arginine-rich proteins (SR proteins) with a characteristic RS domain plays a crucial role in both constitutive and regulated pre-mRNA splicing (Manley and Tacke, 1996; Graveley, 2000; Smith and Valcarcel, 2000). SR proteins are located predominantly in nuclear subdomains referred to as speckles, which function as storage and/or assembly sites for many splicing and transcription components (Sleeman and Lamond, 1999a; Mintz and Spector, 2000; Shopland and Lawrence, 2000). RS domains act as both an NLS and a targeting signal to the splicing speckles, and some of them can direct nucleocytoplasmic shuttling in conjunction with the RNA-binding domains (Hedley *et al*., 1995; Caceres *et al*., 1997; Cazalla *et al*., 2002). SR proteins are imported into the nucleus by importin β-like proteins, transportin-SR (TRN-SR) or its alternatively spliced form TRN-SR2 (Kataoka *et al*., 1999; Lai *et al*., 2000, 2001; Allemand, 2002). Our previous reports have shown that TRN-SR2 interacts specifically with the phosphorylated RS domain derived from ASF/SF2 and mediates the import of phosphorylated SR proteins to the nucleus (Lai *et al*., 2000, 2001). Consistent with this finding, nuclear localization of human SC35 is impaired in yeast when the SR protein kinase homolog Sky1 is deleted (Yeakley *et al*., 1999). Thus, RS domain phosphorylation is important for nuclear import of at least some SR proteins.

In addition to SR proteins, heterogeneous nuclear ribonucleoproteins (hnRNPs) also play a crucial role in modulation of alternative pre-mRNA splicing (Krecic and Swanson, 1999; Smith and Valcarcel, 2000). The hnRNP A1 protein antagonizes the activity of SR proteins on the selection of 5′ splice sites and can bind to certain exon splicing silencers to prevent the use of adjacent 3′ splice sites (Smith and Valcarcel, 2000). Several other hnRNPs, such as F, H and I (polypyrimidine tract-binding protein), modulate pre-mRNA splicing by binding to specific enhancer or silencer elements (Smith and Valcarcel, 2000). Although primarily nuclear, some hnRNP proteins shuttle continuously between the nucleus and the

Table I. Non-SR protein clones selected by yeast two-hybrid screening with N-terminally truncated TRN-SR2 as bait

Clone	No.	Features or motifs
RBM4a	5	RRM, CCHC zinc finger
RBM4b	2	RRM, CCHC zinc finger
ALEX3	4	Armadillo repeats
BAB71287	3	Unknown protein
BAP1	2	Ubiquitin C-terminal hydrolase
MLF2	2	Myeloid leukemia factor 2
ODF2	2	Outer dense fiber of sperm tail 2

The table lists clones that were selected more than twice in the two-hybrid screen. These clones code for non-SR proteins; except for RBM4s, none have been proven to be bona fide TRN-SR2-interacting proteins. No. represents the number of times that the clones were selected.

cytoplasm, implicating their potential roles in RNA export, turnover or translation (Michael, 2000). To date, except for hnRNP A1 whose nuclear import is known to be mediated by transportin (Michael *et al*., 1995), the mechanisms for nuclear transport of the vast majority of hnRNPs still remain to be delineated.

While characterizing TRN-SR2, we identified its novel transport substrate, RNA-binding motif protein 4 (RBM4). RBM proteins constitute a large class of RNA recognition motif (RRM)-containing proteins, but their functions are largely not known. In contrast, an RBM4 homolog, Lark, was previously uncovered in *Drosophila* for its role in the circadian regulation of adult eclosion (McNeil *et al*., 1998). It was postulated that Lark targets to RNA encoding downstream components of the clock output pathway, but the underlying mechanism of how Lark functions is still unknown (Newby and Jackson, 1996). Here we demonstrate that TRN-SR2 specifically interacts with the C-terminal domain of RBM4 and mediates its nuclear import. Interestingly, RBM4 antagonizes the activities of authentic SR proteins on alternative pre-mRNA splicing. Thus, a novel non-SR protein splicing regulator can share an identical import pathway with SR proteins to the nucleus.

Results

Transportin-SR2 interacts with several non-SR proteins in a yeast two-hybrid screen

We previously identified transportin-SR2, an importin β family protein, by its interaction with SR splicing factors (Lai *et al*., 2000). TRN-SR2 recognizes phosphorylated SR proteins and is responsible for their nuclear import (Lai *et al*., 2000, 2001). To search for new ligands that bind to TRN-SR2, we exploited a yeast two-hybrid screening on a HeLa cell cDNA library using N-terminally truncated TRN-SR2 as bait. This screen condition might facilitate selection of transport cargoes of TRN-SR2 because its cargo-binding domain likely locates at the C-terminus, and N-terminal truncation can prevent the interference from nuclear RanGTP. Thirty-six positive clones that activated the reporters only in the presence of the TRN-SR2-fusion bait were characterized; 12 clones encoded SR or SR-like proteins, whereas the remaining coded for non-SR proteins. Table I shows the non-SR protein clones that

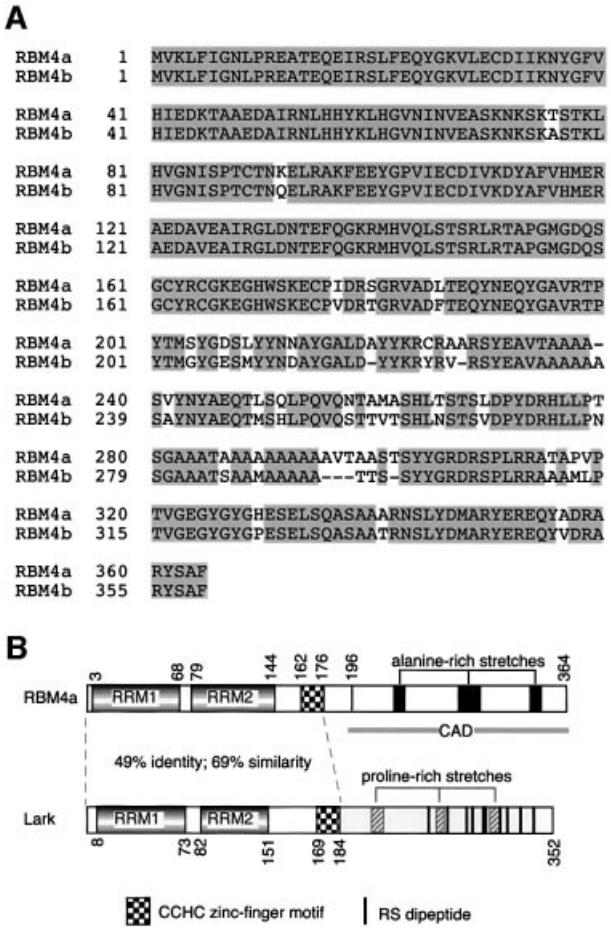

Fig. 1. (**A**) Aligned amino acid sequences of human RBM4a and RBM4b. The sequences are available from DDBJ/EMBL/GenBank under the accession numbers BC000307 for RBM4a and NP_113680 for RBM4b. Shaded are identical residues. (**B**) Schematic representation of the domains of human RBM4a and *Drosophila* Lark.

were selected more than twice in the screen. The encoded proteins included RBM4 proteins, armadillo-repeat containing protein ALEX3, ubiquitin hydrolase BAP1 and several others lacking discernible domains (Table I). These non-SR proteins share no obvious amino acid sequence similarities with each other. Among these potential interacting proteins, we chose RBM4 for further analysis, since it was most frequently isolated in the screening and its RNA-binding domains implies a role in RNA metabolism.

RBM4 proteins are encoded by two different genes

In the above screening, seven out of 24 non-SR-protein clones coded for two different RBM4 proteins (Jackson *et al*., 1997), hereby termed RBM4a and RBM4b, respectively. The two RBM4 proteins are remarkably similar over their entire length (Figure 1A). Mammalian RBM4s are homologous to *Drosophila* Lark at the N-terminal region containing two RNA recognition motifs (RRMs) and a CCHC-type zinc finger, but are highly divergent from Lark at the C-terminal half (Figure 1B). Both RBM4s possess three alanine-rich stretches in the C-terminal region, whereas Lark bears three proline-rich segments and several non-consecutive RS dipeptide

(Figure 1B). The results of BLAST searches revealed that both human *RBM4a* and *RBM4b* genes are situated on chromosome 11q13. The two RBM4 genes are similar in structure, with the coding sequence in exons 2 and 3 (See Supplementary figure 1, available at *The EMBO Journal* Online), indicating evolution of the two genes through gene duplication. However, their untranslated regions (UTRs) share no sequence homology. Alternative splicing events may occur in the 3′ UTR of RBM4b (data not shown), generating at least three splicing variants (Supplementary figure 1). Intriguingly, the entire *RBM4a* gene locates within the *RBM4b* second intron (Supplementary figure 1). Northern blotting using respective 3′UTR as probe showed that expression of the two RBM4 genes was ubiquitous and parallel at their level in human tissues examined (data not shown).

The two RBM4 gene products share a high degree of similarity in sequence, but in this study only RBM4a was selected for further characterization and is referred to as RBM4 hereafter.

RBM4 interacts with TRN-SR2 in vitro

In vitro binding experiments were next carried out to confirm the interaction of RBM4 with TRN-SR2 detected by the yeast two-hybrid system. GST–TRN-SR2 fusion protein was incubated with *in vitro* translated RBM4 and subsequently selected by glutathione–Sepharose. Figure 2A shows that RBM4, like the control ASF/SF2, was pulled down by GST–TRN-SR2 from the reticulocyte lysate (lanes 2 and 6), indicating an interaction of RBM4 with TRN-SR2. Since GTP-bound Ran can dissociate cargo from importin β protein (Mattaj and Englmeier, 1998; Nakielny and Dreyfuss, 1999), we therefore tested whether RanQ69L, which is incapable of hydrolyzing GTP at a significant rate (Klebe *et al*., 1995), could interfere with the binding of RBM4 to TRN-SR2 in the reticulocyte lysate. RanQ69L–GTP, but not Ran–GDP, considerably abolished the binding of RBM4 and ASF to TRN-SR2 (lanes 3, 4, 7 and 8). The result that RBM4 bound to TRN-SR2 in a Ran-sensitive fashion fulfills the authentic criteria for an import receptor–cargo interaction. Thus, RBM4 is likely an import cargo of TRN-SR2.

To determine interaction specificity, importin α and β and transportins were individually fused to GST and tested as possible binding partners for RBM4. Figure 2B shows that ^{35}S-labeled RBM4 bound only to TRN-SR2 but had no significant interactions with the other three import factors. Since several clones of RBM4 identified from the two-hybrid screen lacked a complete N-terminal domain, we further tested whether the C-terminal domain of RBM4 was sufficient for binding to TRN-SR2. The RBM4 C-terminal region encompassing amino acid (aa) residues 196–364 was fused to the maltose-binding protein (MBP). This region contains three alanine-rich stretches, and was thus termed the C-terminal alanine-rich domain (CAD). The fusion protein was produced in bacteria, purified and subsequently subjected to the binding assays. Figure 2C shows that GST–TRN-SR2 pulled down the MBP–CAD fusion, but not MBP alone, suggesting a direct interaction of TRN-SR2 with the CAD of RBM4 (lanes 3 and 4). Consistent with the above observation, GTP-bound RanQ69L efficiently disrupted the interaction of MBP–CAD with TRN-SR2 (lane 6). Moreover, the data indicate that neither post-translational modification of RBM4 nor a transport adaptor, if any provided by reticulocyte lysate, is required for the TRN-SR2–RBM4 interaction.

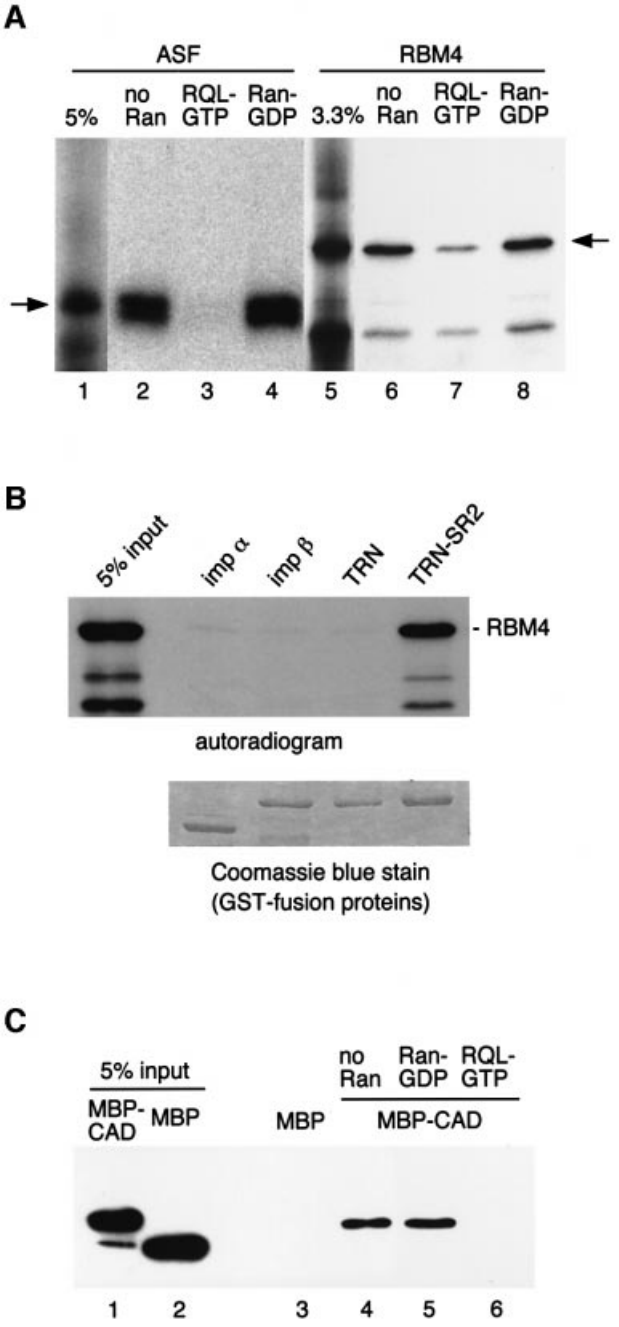

Fig. 2. *In vitro* interaction of RBM4 with TRN-SR2. (**A**) *In vitro* translation reactions (25 μl) containing ^{35}S-labeled ASF (lanes 1–4) or RBM4 (lanes 5–8) were subjected to a pull-down assay using 2 μg (~16 pmol) of GST–TRN-SR2 as the bait. For competition, 80 pmol of RanQ69L–GTP (lanes 3 and 7) or Ran–GDP (lanes 4 and 8) was added. Bound proteins were fractionated by SDS–PAGE followed by autoradiography. Bands corresponding to full-length proteins are designated with arrows. (**B**) GST fusion transport factors were each (2 μg) used to pull down *in vitro* translated RBM4 as in (A). Bound proteins were resolved by SDS–PAGE and subjected to Coomassie Blue staining (lower panel) followed by autoradiography (upper panel). (**C**) Purified MBP or MBP–CAD (~13.5 pmol each) was subjected to pull-down with 2 μg of GST–TRN-SR2. Ran competition was performed as in (A). Bound proteins were detected by immunoblotting using anti-MBP antibodies.

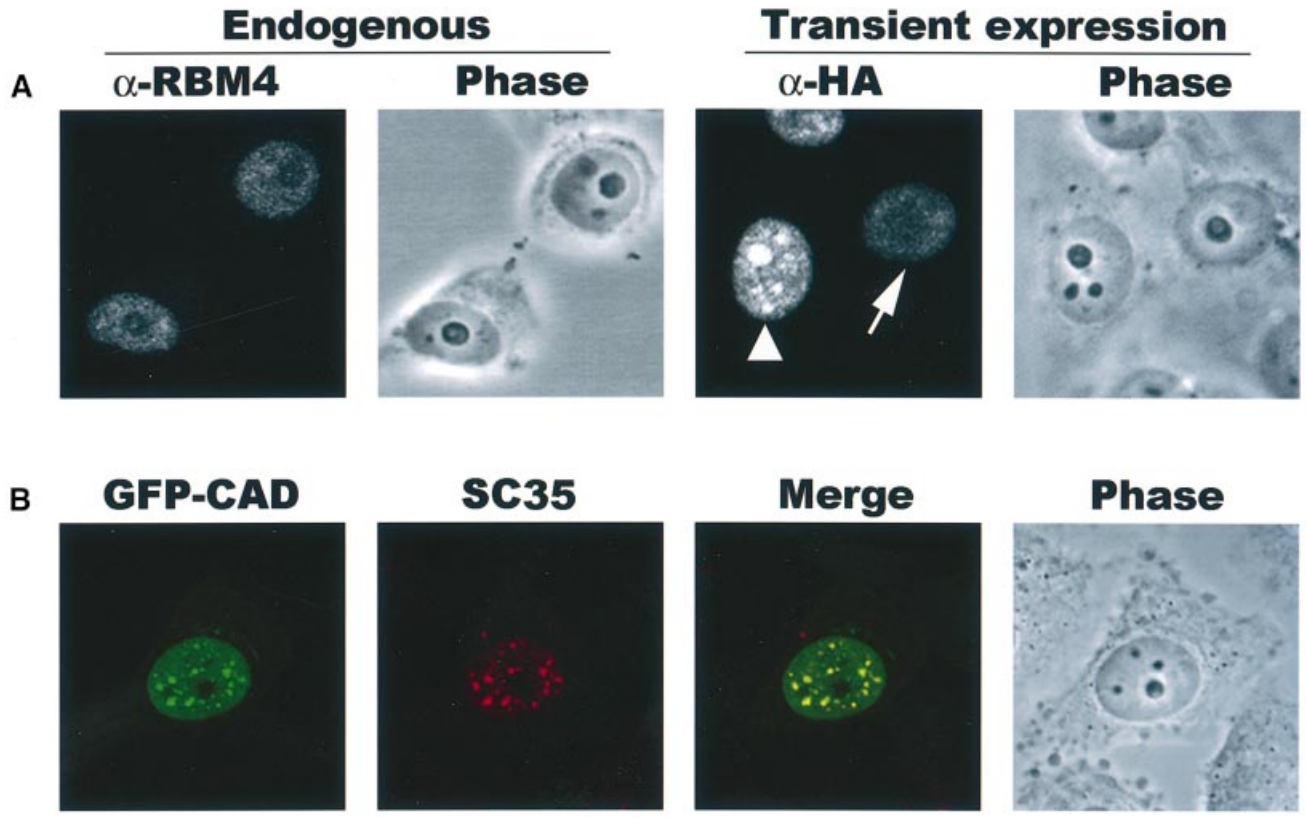

Fig. 3. Cellular localization of RBM4 and a CAD fusion protein. (**A**) Untransfected HeLa cells were stained with anti-RBM4 antibodies (Endogenous), whereas cells transfected with the expression vector of HA-tagged RBM4 were subjected to staining with anti-HA antibody (Transient expression). The arrow indicates an even nucleoplasmic staining pattern of RBM4.HA, whereas the triangle marks the cell where RBM4.HA is concentrated in nucleoli. Cells visualized by phase-contrast microscopy are also shown. (**B**) HeLa cells were transfected with the vector expressing GFP–CAD, and immunostaining with anti-SC35 antibody was performed. Merge: images of fluorescent fusion protein and immunostaining are merged.

The CAD of RBM4 bears the activity of nuclear import and export and speckle targeting

Since the CAD of RBM4 directly interacts with TRN-SR2, we next examined whether the CAD functions as a nuclear localization signal. Initially, we performed indirect immunofluorescence with HeLa cells to determine the steady-state cellular distribution of RBM4. Using purified anti-RBM4 antibodies (see Materials and methods), we observed that endogenous RBM4 distributed evenly in the nucleoplasm as well as at the center of nucleoli (Figure 3A, Endogenous). Transiently-expressed RBM4 bearing a C-terminal hemagglutinin (HA) tag exhibited a similar staining pattern to that of endogenous RBM4 in ~20–30% of transfected cells, whereas in the rest of the cells it showed, intriguingly, highest concentration at the nucleoli in addition to nucleoplasmic distribution (Figure 3A, Transient expression). Nucleolar localization of RBM4 is discussed below.

We next examined whether the CAD of RBM4 could confer complete nuclear localization onto a green fluorescent protein (GFP) reporter when expressed as a fusion protein. GFP alone was detected uniformly within the whole cell (data not shown). Transiently expressed GFP–CAD showed primary localization to the nucleoplasm with, unexpectedly, additional concentration in speckles where SC35 was detected (Figure 3B). This finding indicated that the CAD of RBM4 comprises both nuclear and speckle localization signals, thus sharing a common feature with the RS domain of SR splicing factors (Hedley *et al*., 1995). Protein motifs that target a given protein to specific intranuclear structures are often involved in protein–protein interactions (Eilbracht *et al*., 2001). However, the RBM4 CAD contains neither RS-dipeptide repeats nor a recognizable motif that interacts with known speckle-localized proteins, thus probably representing a novel speckle targeting domain.

RBM4 is localized predominantly in the nucleus, but it could, like many other RNA-binding proteins, undergo continuous nucleocytoplasmic shuttling. To test this possibility, an interspecies heterokaryon assay was performed. In brief, human HeLa cells that transiently expressed HA-tagged RBM4 and a GFP fusion protein as control were fused with mouse NIH 3T3 cells in the presence of cyclohexamide, which inhibits protein synthesis. The heterokaryons were stained for the transfected RBM4 using anti-HA monoclonal antibody. As shown in Figure 4A, both RBM4 and positive control GFP–hnRNP A1 were detected in the mouse nucleus of heterokaryons, whereas non-shuttling GFP–hnRNP C1 was restrained only in the human nucleus. The data thus indicate that RBM4 can rapidly shuttle between the nucleus and the cytoplasm.

Finally, we examined whether the CAD bears nuclear export activity. Heterokaryons were formed by fusion of

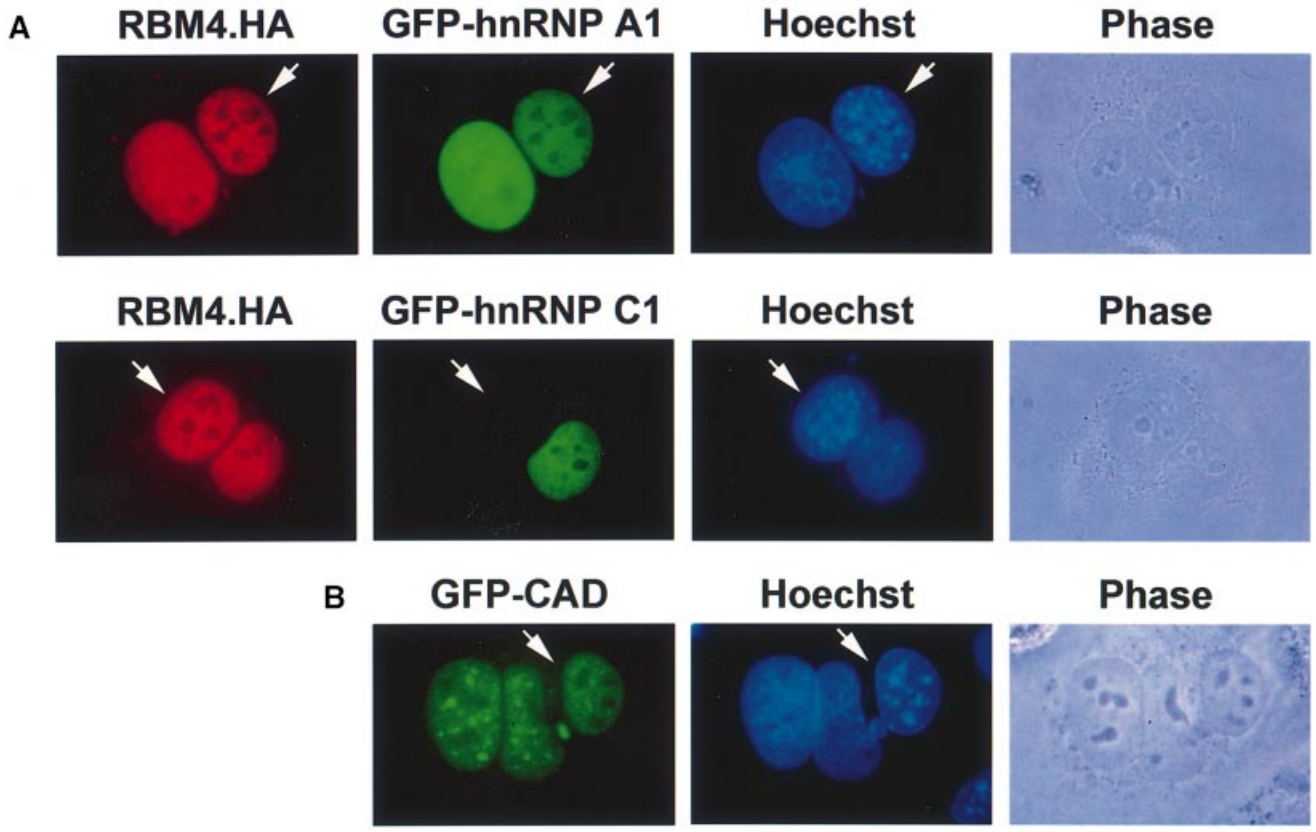

Fig. 4. Interspecies heterokaryon analysis of RBM4 and a CAD fusion protein. (**A**) HeLa cells were co-transfected with vectors for HA-tagged RBM4 and GFP–hnRNP A1 or GFP hnRNP C1 as nucleocytoplasmic shuttling and non-shuttling control, respectively. Heterokaryons were formed and analyzed as described in Materials and methods. Mouse nuclei (arrows) of heterokaryons were distinguished by Hoechst 33258 staining. Phase: phase-contrast image of the heterokaryons. (**B**) A heterokaryon assay was performed by fusion of HeLa cells that transiently expressed GFP–CAD with NIH 3T3 cells.

HeLa cells that transiently expressed GFP–CAD with NIH 3T3 cells. GFP–CAD was detected in the mouse nucleus of heterokaryons (Figure 4B). Since the levels of GFP–CAD in nuclei of both species were comparable, it is unlikely that residual GFP–CAD, if any, in the HeLa cell cytoplasm, directly entered into mouse nuclei after cell fusion. Thus, the CAD may also serve as a nuclear export signal, and is analogous to the M9 domain of hnRNP A1 (Michael *et al*., 1995).

TRN-SR2 mediates the nuclear import of a CAD-bearing protein

Although the CAD of RBM4 has both import and export activities, its interaction with TRN-SR2 was Ran-sensitive. We therefore went on to characterize the mechanism of CAD-mediated nuclear import and to investigate whether TRN-SR2 is involved. Import assays were performed *in vitro* in digitonin-permeabilized HeLa cells by using the recombinant MBP–CAD protein as the transport substrate. Nuclear import of the fusion protein was subsequently monitored by indirect immunofluorescence with anti-MBP antibody. As with the fluorescein-labeled BSA–NLS control, MBP–CAD entered the nuclei of permeabilized cells in the presence of the HeLa cell cytoplasmic extract (cytosol) as a source of transport factors and an ATP-regenerating system (Figure 5A). MBP alone failed to localize to the nucleus under the same conditions (data not shown). Moreover, nuclear entry of MBP–CAD was blocked by wheatgerm agglutinin, an established inhibitor of facilitated nuclear translocation (data not shown), suggesting that its import is in a transport factor-assisted manner. When the import reactions were carried out on ice, nuclear uptake of MBP–CAD was substantially reduced, but not completely blocked (Figure 5A). This result was in part reminiscent of that observed with the GST–RS domain fusion whose nuclear import can take place at low temperature (Lai *et al*., 2001), albeit with higher efficiency than MBP–CAD.

Since RBM4 bound specifically to TRN-SR2 among several nuclear transporters (Figure 2), we subsequently performed competition assays to determine whether its import employs a pathway used by SR proteins. For these experiments, GST–SV40 NLS conjugate or GST fusion to M9 or RS domain was used as competitor at an excess of at least 40-fold molar over the substrate. Since recombinant SR proteins require phosphorylation for efficient nuclear import (Lai *et al*., 2001), GST–RS was phosphorylated *in vitro* by SRPK1 prior to use in the competition assay. Figure 5A shows that phosphorylated GST–RS abolished MBP–CAD nuclear import, whereas GST or its NLS conjugate or M9 fusion had no significant effect. This result suggested that RBM4 and SR proteins share at least one limiting transport factor for nuclear import.

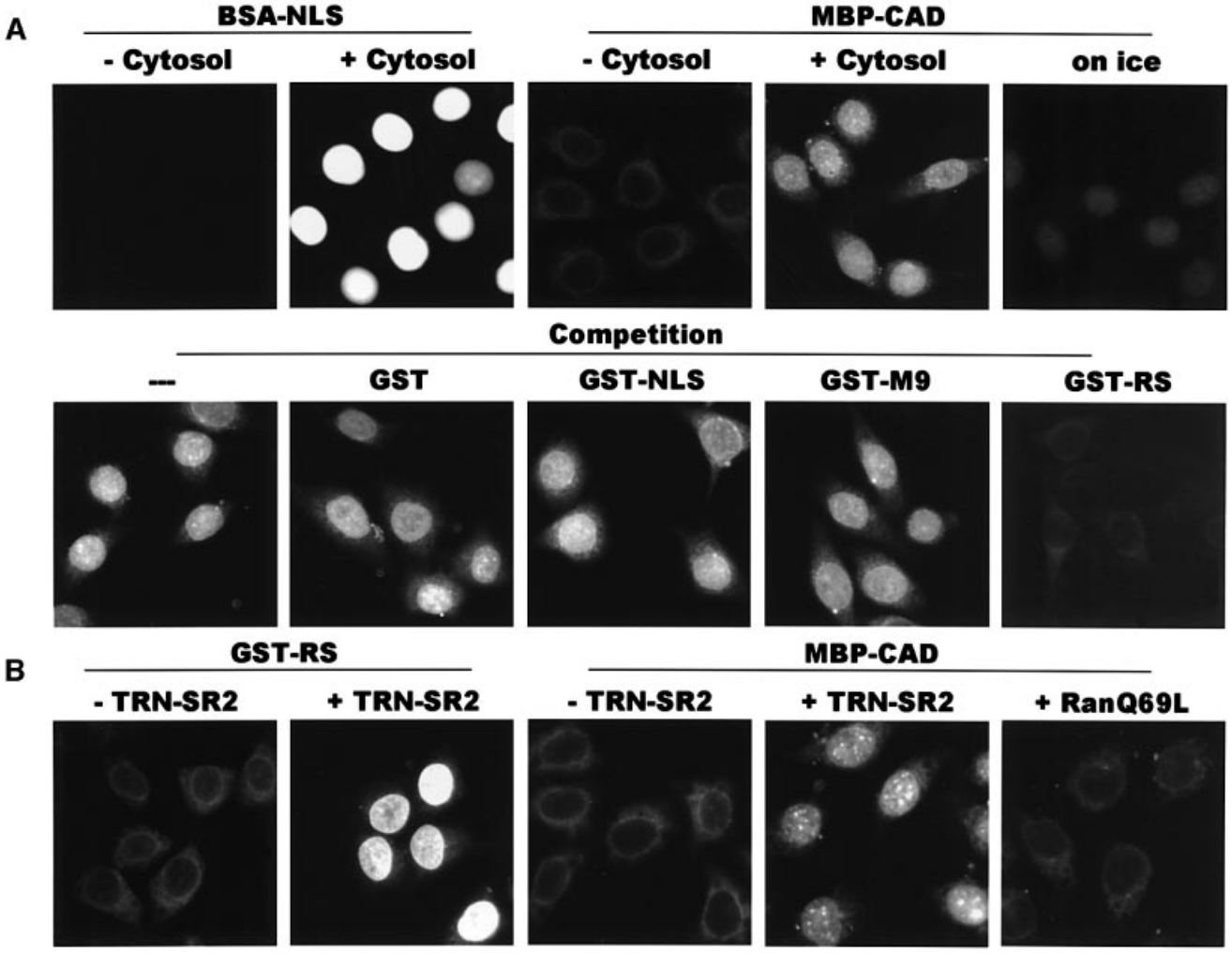

Fig. 5. Nuclear import of an RBM4 CAD fusion protein in permeabilized HeLa cells. (**A**) Fluorescein-labeled BSA-SV40 NLS or MBP–CAD was incubated with permeabilized HeLa cells in the presence (+) or in the absence (–) of HeLa cell cytoplasmic extract (cytosol) at 30°C for 30 min. Import of MAP–CAD was also examined by incubation on ice. Competition was performed in the presence of GST or GST conjugate or fusion proteins at ⩾40-fold molar excess over MBP–CAD. (**B**) The reconstituted import assays for GST–RS and MBP–CAD proteins were carried out in a bacterial extract containing TRN-SR2 (+TRN-SR2) or in mock extract (–TRN-SR2). The effect of RanQ69L–GTP (0.1 mg/ml) on import of MBP–CAD was examined. Detection of MBP–CAD and GST–RS was performed by indirect immunofluorescence with anti-MBP and anti-GST antibody, respectively.

Finally we examined whether TRN-SR2 indeed serves as an import transporter for RBM4. Bacterial lysate containing TRN-SR2 and supplemented with purified Ran and NTF2 (Lai *et al*., 2001) was used in the reconstituted import assay. Like GST–RS, nuclear import of MBP–CAD was observed in the presence of TRN-SR2, but not detected when bacterial lysate without TRN-SR2 was used (Figure 5B). As expected, addition of GTPase-deficient mutant RanQ69L blocked the import, most likely by preventing the binding of TRN-SR2 to MBP–CAD (Figure 5B). Together, our results support the hypothesis that TRN-SR2 mediates the nuclear import of a CAD-bearing protein. Furthermore, it is noteworthy that MBP–CAD accumulated in the nucleus as dots, reminiscent of the accumulation of unliganded TRN-SR2 in nuclear speckles (Lai *et al*., 2001). This also echoed the above observation that the RBM4 CAD was capable of targeting protein to nuclear speckles (Figure 3).

RBM4 modulates alternative 5′ splice site and exon selection in vivo

Since RBM4 is a nuclear RNA-binding protein and shares an identical import pathway with SR proteins to the nucleus, we next set out to determine whether RBM4 functions in pre-mRNA splicing. We initially tested whether RBM4 could modulate alternative 5′ splice site selection *in vivo* by cotransfection of an RBM4 expression vector with the adenovirus E1A reporter (Figure 6A; Caceres *et al*., 1994). To assay E1A pre-mRNA splicing, the E1A RNA products were amplified by RT–PCR and subsequently detected by hybridization with a ^{32}P-labeled primer complementary to the 3′ exon. Transient transfection of the E1A construct alone resulted in multiple mRNA isoforms that represent alternative 5′ splice site utilization (Figure 6B, lane 1). Cotransfection of the ASF/SF2 cDNA promoted splicing of the E1A pre-mRNA at the 13S 5′ splice site (lane 2), as reported (Caceres *et al*., 1994). In

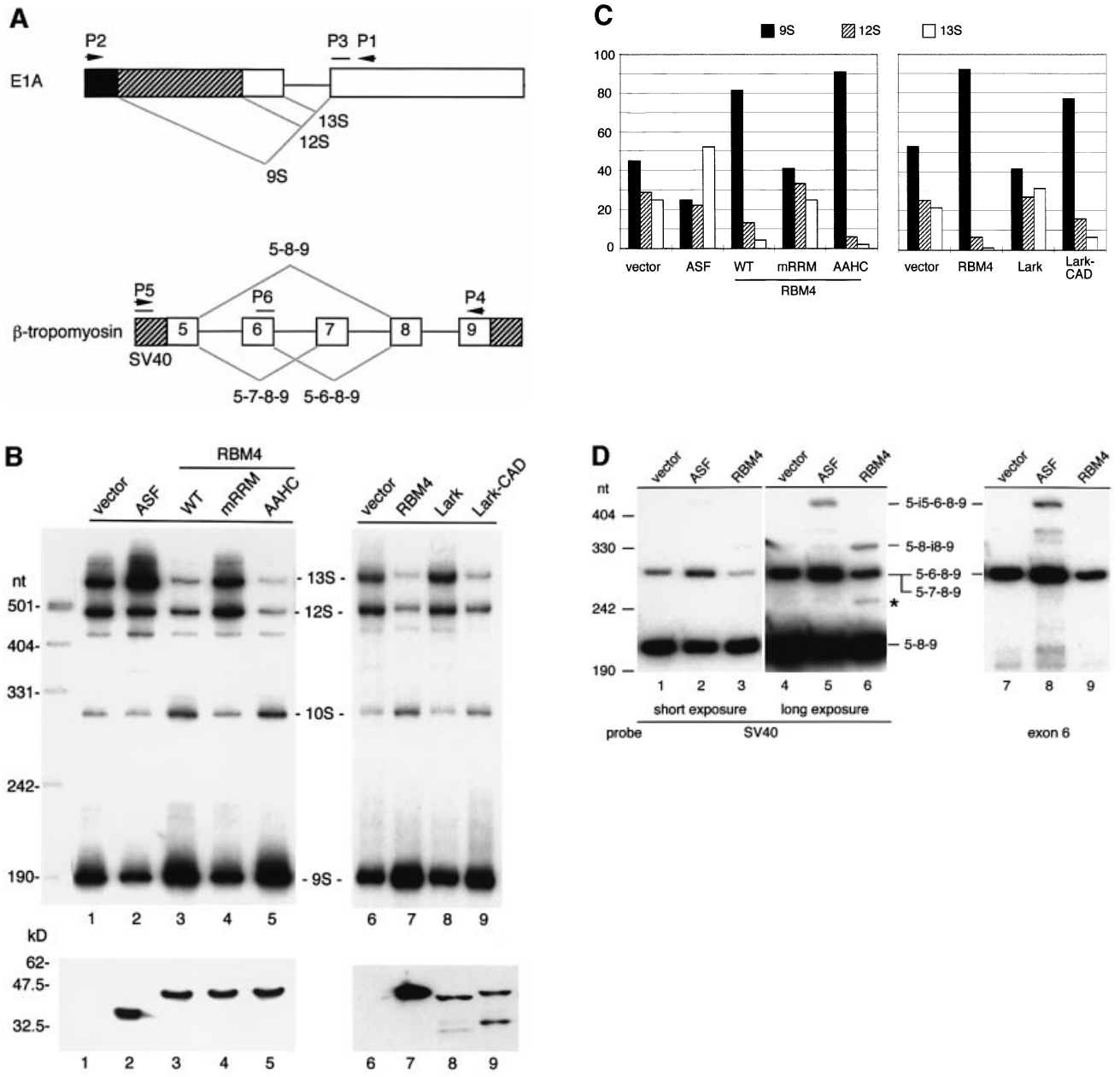

Fig. 6. Effect of RBM4 on *in vivo* alternative pre-mRNA splicing. (**A**) The diagrams show the adenovirus E1A pre-mRNA (upper panel) and the rat β-tropomyosin minigene (lower panel), and their major splicing products. The arrows and solid lines denote primers for RT–PCR and hybridization, respectively. Hatched boxes in the tropomyosin minigene are the SV40 sequences. (**B**) *In vivo* splicing assays were performed with HeLa cells transiently co-transfected with the E1A reporter and expression vector of HA-tagged effector as indicated. Total RNA was isolated and subjected to RT–PCR with P1 and P2, and the splicing products were analyzed by hybridization with ^{32}P-labeled probe P3. pUC19/MspI DNA size markers are shown with lengths in nucleotides on the left. Western blotting with anti-HA antibody was used to detect HA-tagged effector proteins (lower panel). Protein size markers are indicated on the left. (**C**) The blots of (B) were subjected to a quantitative analysis using a PhosphorImager. The relative abundance of the major splicing products is shown as a percentage. (**D**) HEK 293 cells were transiently co-transfected with the β-tropomyosin minigene plasmid and expression vector of HA-tagged ASF or RBM4. Analysis of splicing products was as in (B), except for the use of P4 and P5 in RT–PCR. Hybridization was performed with primer P5 (SV40), and the blot was subjected to autoradiography (lanes 1–3, short-time exposure; lanes 4–6, long-time exposure). The same blot was stripped and rehybridized with primer P6 (exon 6; lanes 7–9). The identity of the band marked by the asterisk is not determined.

contrast, increased expression of RBM4 predominantly generated the 9S mRNA and additionally suppressed the use of the two proximal sites (lane 3). RBM4 thus had preference for the most distal 5′ splice site and exhibited an opposite effect to ASF/SF2 in 5′ splice site selection of the E1A pre-mRNA (Figure 6C).

We furthermore tested the effect of RBM4 overexpression on alternative splicing of rat β-tropomyosin pre-mRNA that is regulated in a tissue-specific manner (Caceres *et al.*, 1994 and references therein). The β-tropomyosin minigene construct was cotransfected with expression vector for ASF or RBM4 into HEK 293

cells. Splicing of the tropomyosin pre-mRNA was determined by RT–PCR followed by hybridization with specific probes. Transient expression of the β-tropomyosin minigene alone yielded two bands detected by the SV40 primer, one corresponding to co-migrated fibroblast-specific form 5-6-8-9 and skeletal muscle-specific form 5-7-8-9 and the other corresponding to the 5-8-9 mRNA of which both exons 6 and 7 are skipped (Figure 6D, lane 1). Overexpression of ASF/SF2 stimulated inclusion of exon 6 or 7 by ~2-fold, and concomitantly decreased the level of the 5-8-9 mRNA (lane 2). In contrast, the level of exon 6- or 7-containing transcripts slightly declined upon overexpression of RBM4 although that of the 5-8-9 mRNA remained largely unchanged (lane 3). Further analysis using a specific primer to exon 6 (lanes 7–9) or exon 7 (data not shown) confirmed that RBM4 prevented inclusion of exon 6 or 7 while overexpressed, and thus acted in an opposite way to ASF/SF2. In addition, ASF/SF2 or RBM4 overexpression induced intron retention, thus resulting in the production of 5-i5-6-8-9 and 5-8-i8-9 transcripts, respectively (lanes 5 and 6). Yet it is unclear whether these intron-retained products are only splicing intermediates or not, but this result further indicated that ASF/SF2 stimulated inclusion of exon 6 whereas RBM4 preferred to exclude it.

Next we generated RBM4 mutants to examine the domain(s) mediating 5′ splice site selection of the E1A pre-mRNA. RBM4 with mutations at the conserved aromatic amino acid residues of the RRMs was unable to switch the E1A 5′ splice site utilization (Figure 6B; lane 4). This did not result from poor yield or abnormal subcellular localization of the mutant protein since this protein was expressed at a comparable level to that of the wild type (Figure 6B, bottom) and localized in the nucleus (Supplementary figure 2, mRRM). In contrast, the mutation introduced in the CCHC-type zinc finger motif had no effect on the splice site switch activity of RBM4 (lane 5). Furthermore, we investigated whether the CAD domain plays any role in alternative pre-mRNA splicing. Deletion of the CAD abolished E1A splice site switch to the 9S site (data not shown), but incomplete nuclear entry of the truncated protein (Supplementary figure 2, ΔCAD) made interpretation of the data difficult. We thus thought to test the activity of the *Drosophila* RBM4 homolog, Lark protein, on alternative splicing. The Lark protein shares ~70% similarity with RBM4, but only at the N-terminal half (Figure 1B). Overexpression of Lark did not induce 5′ splice site switch of the E1A pre-mRNA (Figure 6B, lane 8). Interestingly, the chimeric protein encompassing the N-terminal domain of Lark and the RBM4 CAD considerably activated the utilization of the 9S site although its expression was relatively low (lane 9). This result indicated that the CAD contributes significantly to the splice site switch activity of RBM4. The RRM domain is nevertheless necessary since the GFP–CAD fusion failed to switch the splice site utilization (data not shown).

In vitro function of RBM4 in alternative pre-mRNA splicing

We next analyzed whether recombinant RBM4 protein could modulate alternative splicing *in vitro*, using a model adenovirus major late (AdML) pre-mRNA that possesses alternative 5′ splice sites (Figure 7, top; Tarn and Steitz, 1994). Splicing of the AdML pre-mRNA occurred at the distal 5′ splice site when the reaction was carried out in the HeLa cell nuclear extract or in the cytosolic S100 extract complemented with limiting amounts of a mixture of SR proteins (Figure 7, lanes 1 and 3). Elevated concentrations of SR proteins activated the splicing at the proximal 5′ splice site and concurrently suppressed the use of the distal site (lanes 4 and 5). His-tagged RBM4 protein purified from *Escherichia coli* lysate was titrated in the S100 extract supplemented with excess SR proteins, showing that RBM4 was capable of shifting splicing in favor of the distal 5′ splice site in a dose-dependent manner (lanes 7–10). The eluate from the mock-transformed *E.coli* lysate had negligible effect (lane 6). To evaluate the role of RRMs in splice site switch, recombinant RBM4 protein bearing mutations at the RRMs and MBP–CAD lacking the entire RRMs were tested. Neither of these proteins was able to counteract the activity of SR proteins (lanes 16 and 17), thus consistent with the *in vivo* observation that the RRM domain plays a critical role in modulation of alternative 5′ splice site utilization.

The above data indicate that RBM4 is a novel splicing regulator that modulates alternative splice site selec tion. Next, to address whether RBM4 plays any role in

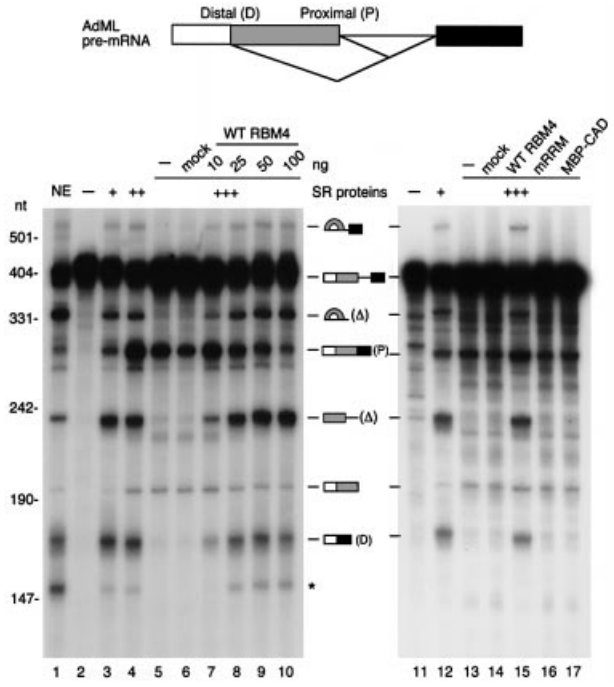

Fig. 7. Effect of RBM4 on *in vitro* splicing of the adenovirus major late (AdML) pre-mRNA. The top diagram shows the AdML pre-mRNA and splicing products. Splicing was carried out in HeLa cell nuclear (lane 1) or S100 extract (lanes 2 and 11), or S100 extract supplemented with SR proteins (lanes 3 and 12, 0.15 μg; lane 4, 0.3 μg; lanes 5–10 and 13–17, 0.6 μg). In addition, the reactions contained increasing amounts of purified wild-type RBM4 (lanes 7–10), 50 ng wild-type (lane 15), 100 ng RRM mutant RBM4 (lane 16) or 100 ng MBP–CAD (lane 17). The mock fraction containing no recombinant protein was added as control (lanes 6 and 14). Size markers are given on the left. Pre-mRNA and splicing intermediates and products are depicted in the middle. Note that mRNA (D) generated by the use of the distal 5′ splice site is susceptible for degradation in extract as described elsewhere (Tarn and Steitz, 1994; a degraded fragment denoted by the asterisk). However, the levels of the intron (triangles) excised by splicing at the distal site obviously elevated with increasing amounts of RBM4 (lanes 7–10).

constitutive pre-mRNA splicing, we attempted to deplete RBM4 from HeLa cell nuclear extract. While a substantial amount of RBM4 protein(s) was depleted with anti-RBM4 antibodies, splicing of the AdML pre-mRNA was not affected (Supplementary figure 3). Thus, RBM4 may not be critical for constitutive pre-mRNA splicing, but whether a limited amount of RBM4 was sufficient for splicing or whether RBM4b could complement the splicing defect, if any, of RBM4a-depleted extract is unclear. The role of RBM4 in pre-mRNA splicing certainly needs further investigation.

Discussion

Nucleocytoplasmic transport is a dynamic activity and involves multiple and complex pathways. Many nuclear transport receptors and their first cargoes have been characterized to date, but a more complete picture of how transport diversity is achieved is still lacking. Here we identify a novel TRN-SR2 cargo, RBM4, that harbors no RS dipeptide repeats, thus adding a new repertoire for TRN-SR2-mediated nuclear import.

Although, at present, the subregions of RBM4 that interact directly with TRN-SR2 have not been defined, the CAD neither contains RS repeats nor undergoes extensive phosphorylation and is thus conceivably divergent from RS domains. Other importin β family members, such as importin β and transportin, can also import protein cargos with diverse signals (Siomi *et al*., 1997; Jakel and Gorlich, 1998). Importin β achieves this by employing different adaptor molecules, interacting with another importin β family protein, or through separable binding sites (Huber *et al*., 1998; Jakel and Gorlich, 1998; Jakel *et al*., 1999; Jullien *et al*., 1999). The interactions of TRN-SR2 with both RBM4 and SR proteins do not necessarily involve any adaptor factors (Figure 2) and are all via the TRN-SR2 C-terminal domain (data not shown). Therefore, how TRN-SR2 recognizes these very different signals needs further investigation. Moreover, phosphorylation of the ASF RS domain greatly increases its affinity with TRN-SR2 (Lai *et al*., 2000). In contrast, post-translational modification, if any, appears not to be critical for the RBM4 CAD interaction with TRN-SR2 and its subsequent nuclear import (Figures 2 and 5). Furthermore, a recent report proposes that multiple receptors binding to a cargo can synergistically enhance the efficiency of translocation through NPC (Ribbeck and Gorlich, 2002). It is reasonable to conceive that RS domains comprise multiple, separate or overlapping segments of RS repeats, thereby binding to more than one TRN-SR2. If this is true, import of SR proteins might be more efficient than that of the cargo bound by only one molecule of TRN-SR2. Nevertheless, whether RBM4 harbors more than one signal for TRN-SR2 or for other importin β members awaits to be examined.

RBM4 is mainly distributed in the nucleoplasm, but its CAD can localize a heterologous protein to the nuclear speckles (Figure 3). This intriguing result echoes our previous hypothesis that TRN-SR2 is capable of escorting its cargoes to nuclear speckles (Lai *et al*., 2001). Speckles are characterized by high concentrations of pre-mRNA splicing factors including SR proteins and snRNPs (Mintz and Spector, 2000). In addition to these proteins that locate more steadily at splicing speckles, a recent report shows that newly synthesized NHPX is transiently localized to speckles prior to its destination to nucleoli (Leung and Lamond, 2002). By examining RBM4 distribution at different stages of mitosis, we observed that ectopically expressed GFP–full-length RBM4 fusion accumulated with SC35 in speckles immediately following the reformation of the nuclear envelope and subsequently dispersed (data not shown). This supports the idea that newly imported RBM4 is probably targeted to speckles via its CAD-mediated pathway before redistribution to other subnuclear compartments. RBM4 became accumulated in the nucleoli while overexpressed (Figure 3), but its nucleolar localization was abolished by inhibition of transcription (data not shown) or by RRM mutations (Supplementary figure 2). RBM4 was also detected in nucleoli by a recent proteomic analysis of proteins that are associated transiently with nucleoli or under specific metabolic conditions (Andersen *et al*., 2002). Thus, whether RBM4 could temporarily localize to the nucleoli and whether intranuclear trafficking of RBM4 involves specific directional pathways like that of snRNPs and NHPX (Sleeman and Lamond, 1999b; Sleeman *et al*., 2001; Leung and Lamond, 2002) will require investigations in the future.

RBM4, a novel pre-mRNA splicing regulator, can modulate the selection of alternative 5′ splice sites or exons upon overexpression (Figure 6) and antagonizes the effect of SR proteins on 5′ splice site choice *in vitro* (Figure 7). RBM4 thus behaves in this aspect like hnRNP A1. The usage of alternative splice sites is often influenced by competitive binding of SR proteins and hnRNPs (Smith and Valcarcel, 2000). No significant interaction between RBM4 and SR proteins was detected in a protein overlay assay (data not shown), making the possibility that RBM4 simply sequesters SR proteins less likely. Previous studies have revealed distinct mechanisms used by hnRNP A1 in modulation of alternative splicing. For example, excess hnRNP A1 can disturb 5′ splice site occupancy by U1 snRNP and thereby activates the sites with high affinity to U1 for use (Eperon *et al*., 2000). In addition, hnRNP A1 can bind to exonic or intronic elements to cause exon skipping (Blanchette and Chabot, 1999). Whether RBM4 functions in a similar manner as hnRNP A1 needs further examination. In this study, we have demonstrated that both RRM and CAD domains of RBM4 are critical in modulating splice site selection (Figures 6 and 7). The possibility of whether the CAD of RBM4 acts as a protein interaction module and thereby interacts with other splicing factors to participate in splicing regulation remains to be examined. Moreover, it would be of interest to investigate whether RBM4 possesses any RNA binding specificity through its RRMs and/or zinc finger and thereby modulates splice site choice of specific pre-mRNAs.

Earlier studies by transient expression of individual splicing regulators have revealed that the relative abundance of antagonistic factors can determine splice site utilization (Caceres *et al*., 1994). Analogously, our data indicate that the relative amounts of RBM4 and SR proteins also influence the outcome of alternative splicing (Figures 6 and 7). More interestingly, these antagonistic splicing regulators are imported to the nucleus via the same TRN-SR2-mediated pathway. A recent report shows that *Drosophila* repressor splicing factor 1 (RSF1), an SR-like

protein, can counteract the activity of ASF/SF2 in splicing and its nuclear import is also mediated by dTRN-SR (Allemand *et al*., 2002). Thus, TRN-SR2 can import various splicing regulators to the nucleus, but the question of whether TRN-SR2 could alter their relative concentration and thereby impact on alternative pre-mRNA splicing still remains to be tested. Evidence has been provided recently that nuclear abundance of splicing regulators can be altered upon physiological stimuli (van der Houven van Oordt *et al*., 2000). Stress stimuli induce phosphorylation and cytoplasmic accumulation of hnRNP A1 via the $MKK_{3/6}$–p38 signaling pathway, leading to a distinct alternative splicing pattern of the E1A pre-mRNA. Therefore, it would be of additional interest to detect whether any cellular stimuli could directly target to TRN-SR2 or other transport factors, thus varying the concentration of their cargoes in the nucleus and controlling splice site selection of alternative splicing.

Materials and methods

Yeast two-hybrid screening

The DNA fragment corresponding to N-terminally truncated TRN-SR2 (ΔN281; Lai *et al*., 2000) was cloned into plasmid pAS2-1 (Clontech) and then used as the bait to screen a HeLa cell cDNA library (Clontech). Yeast transformation and screening were performed as described in the protocol provided by the manufacturer. Putative positive clones were verified by cotransformation with the bait plasmid into yeast, and their sequences were analyzed.

Plasmid constructions

The cDNAs encoding full-length RBM4 were obtained by RT–PCR using total RNA prepared from HeLa cells as template. The entire RBM4 coding region was cloned into pGEM-3Z (Promega), pQE-82L (Qiagen) and pCEP4 (Invitrogen); the latter two plasmids express His_6-tagged and HA-tagged RBM4, respectively. The C-terminal region (CAD; aa 196–364) of RBM4 was inserted in-frame into pEGFP-C1 (Clontech) and pMAL-c2 (NEB); the resulting plasmids produce GFP–CAD and MBP–CAD, respectively. The QuikChange site-directed mutagenesis system (Stratagene) was adopted to make RBM4 mutants. The mRRM mutant contained four mutations (Y37A, F39A, Y113A and F115A) in the RRM domain, whereas AAHC had two mutations, C162A and C165A, in the zinc finger. Moreover, the Lark cDNA was amplified by PCR using a *Drosophila* embryonic cDNA library (gift of H.Sun, Academia Sinica, Taipei, Taiwan). The Lark–CAD fusion was designed to contain aa 1–184 of Lark and aa 177–364 of RBM4. For RBM4 mutants, Lark and Lark–CAD chimera, each corresponding DNA fragment was amplified and subcloned into pCEP4 and/or pQE-82L.

The plasmids pGEX-importin α and β were generous gifts of Y.Yoneda (Osaka University, Osaka, Japan). The transportin cDNA (from J.Steitz, Yale University, New Haven, CT) was amplified by PCR and inserted in-frame into pGEX-2T (Amersham Pharmacia Biotech). The DNA fragments corresponding to ASF RS domain (aa 195–248) and hnRNP A1 M9 domain (aa 264–308) were also inserted into pGEX-2T.

Recombinant proteins and preparation of anti-RBM4 antibodies

The MBP–CAD protein was produced in *E.coli* strain BLR and purified over maltose–Sepharose beads according to the manufacturer's instructions (NEB). GST or GST fusion proteins (GST–RS, –M9, –importin α, –importin β family proteins) were overexpressed in *E.coli* strain XA90 or BLR and purified using glutathione–Sepharose beads (Amersham Pharmacia Biotech). His-tagged wild-type and mRRM RBM4 proteins were overexpressed in *E.coli* strain BLR. The lysate was loaded onto nickel agarose (Novagen), and bound proteins were step-eluted with increasing concentration (0.2, 0.4 and then 1 M) of imidazole. The 1 M imidazole eluate was dialyzed against buffer D (Mayeda and Krainer, 1999) and used in the *in vitro* splicing assays (see below). Recombinant Ran and RanQ69L were purified and charged with appropriate nucleotides as described in Lai *et al*. (2000). To raise anti-RBM4 serum, rabbits were immunized with purified His-RBM4. Anti-RBM4 antibodies were affinity-purified over GST–RBM4-conjugated Sepharose beads, and recognized a major band of ~42 kD on an immunoblot of HeLa cell extract.

In vitro pull down assay

GST fusion transport factors (2 μg each) were each incubated with 25 μl *in vitro* translated or 2 μg recombinant cargo protein in a 60 μl mixture at 30°C for 30 min. For competition, 2 μg of RanQ69L–GTP or Ran–GDP was added. The reaction mix was subsequently incubated with 10 μl glutathione–Sepharose at 4°C for 2 h. Bound proteins were extracted with SDS lysis buffer and analyzed by autoradiography for *in vitro* translated proteins or by immunoblotting for MBP fusion cargoes using anti-MBP antibody (NEB).

In vivo splicing

The E1A expression vector (pCEP4-E1A; 0.67 μg) was co-transfected with pCEP4-derived vectors encoding effector protein (1.33 μg) into HeLa cells grown to 60–70% confluency in a 35 mm dish. At 30 h post-transfection, total RNA was isolated using Trizol reagent (Gibco BRL) and treated with RQ-DNase I (Promega). RT was performed using primer P1 (5′-GGTCTTGCAGGCTCCGGTTCTGGC), and the following PCR was performed with primers P1 and P2 (5′-GCAAGCTTGAGTGC-CAGCGAGTAG). One-twentieth volume of the PCR mixtures was fractionated on a 6% denaturing polyacrylamide gel and transferred onto a nylon membrane. The blots were probed with ^{32}P-labeled oligonucleotide P3 (5′-CTCAGGCTCAGGTTCAGACACAGG) using standard methods followed by autoradiography and quantitative analyses using a PhosphorImager (Molecular Dynamics).

The β-tropomyosin minigene plasmid pSV40-p2 (0.67 μg; gift of A.Krainer, Cold Spring Harbor Laboratory, Cold Spring Harbor, NY) was co-transfected with an effector expression vector (1.33 μg) into HEK 293 cells in a 35-mm dish. RNA preparation was the same as above. RT was performed using P4 (5′-TTTGCCACAGATCTTTCAGC), and PCR was carried out with P4 and P5 (5′-TTTTGGAGGCCTAGGCTTTT). Analysis of PCR products was analogous to the above, except that primer P5 or P6 (5′-GAGGAGCTTCGAACCATGGACC) was used for hybridization. The intron-containing products were gel-eluted and cloned for sequence analysis.

In vitro splicing

HeLa cell nuclear and S100 extracts were prepared as described in Mayeda and Krainer (1999). Mixed SR proteins were isolated from frozen HeLa cell nuclei (Cell Culture Center) using a method described by Zahler *et al*. (1992). Preparation of ^{32}P-labeled AdML pre-mRNA and *in vitro* splicing reactions in 25 μl were essentially as described (Tarn and Steitz, 1994), except that 40 instead of 60% nuclear or S100 extract was used in splicing. RNA products were analyzed by electrophoresis on a 7% denaturing polyacrylamide gel.

Indirect immunofluorescence and heterokaryon assay

Indirect immunofluorescence was carried out as described in Lai *et al*. (1999). The primary antibodies used were affinity-purified anti-RBM4 antibodies (0.5 μg/ml), monoclonal anti-SC35 antibody (3 μg/ml; Sigma), or monoclonal anti-HA antibody (gift of S.-C.Cheng, Academia Sinica, Taipei, Taiwan). Fluorescein-conjugated anti-rabbit IgG (20 μg/ml; Cappel Laboratory) or Texas Red-conjugated anti-mouse IgG (2 μg/ml; Cappel Laboratory) were used as secondary antibodies.

For heterokaryon assays (Michael *et al*., 1995), HeLa cells were co-transfected with the RBM4.HA-expressing vector and pEGFP-hnRNP A1 or pEGFP hnRNP C1 (kind gifts of J.Lykke-Andersen; University of Colorado, Boulder, CO) or transfected with pEGFP-CAD alone for 36 h. NIH 3T3 cells were then added to the HeLa cells. The co-cultures were treated with cyclohexamide (Sigma) at a concentration of 50 μg/ml for 3 h and 100 μg/ml for another 30 min. The cells were then treated with 50% polyethylene glycol 3350 (Sigma) for 2 min to induce fusion, and subsequently returned to fresh media containing 100 μg/ml cyclohexamide for 3 h. Indirect immunofluorescence using anti-HA antibody was performed to locate HA-tagged RBM4 as above. The cells were also counterstained with Hoechst 33258 (Sigma) to distinguish HeLa from mouse NIH 3T3 cells.

In vitro import assay

Permeabilization of HeLa cells and *in vitro* import reactions were performed essentially as described in Lai *et al*. (2001). In brief, 20 μl import reactions containing 5 μl HeLa cell cytoplasmic extract, 1 μg MBP–CAD and an energy regeneration system were incubated with permeabilized cells at 30°C for 30 min. For competition, 20 μg of GST or GST fusion proteins, or 6 μg of GST–NLS conjugate (approximately five

molecules of the peptide per GST molecule) was added. For reconstituted import assays, 8 µl TRN-SR2-containing *E.coli* lysate (Lai *et al*., 2001), 1.5 µg Ran–GDP and 0.2 µg NTF2 were added to the reactions. As import substrate or competitor, GST–RS was *in vitro* phosphorylated by GST–SRPK1 as described (Lai *et al*., 2001). The synthetic SV40 NLS peptide (CGGGPKKKRKVED) was conjugated to GST or fluorescein-labeled BSA as described in Lai *et al*. (2001). To monitor nuclear import of MBP–CAD, indirect immunofluorescence was carried out using anti-MBP antibody (1 µg/ml; NEB).

Supplementary data

Supplementary data are available at *The EMBO Journal* Online.

Acknowledgements

We are grateful to Drs J.Steitz, Y.Yoneda, A.Krainer, S.-C.Cheng, H.Sun and J.Lykke-Andersen for the generous gifts of plasmids and antibodies, and to M.Shu and J.-C.Lin for technical assistance. We thank Drs F.-J.Lee and Y.-S.Lin for critical reading of the manuscript. This work was supported by Academia Sinica and Grant NSC90-2311-B-001-147 from the National Science Council of Taiwan.

References

Allemand,E., Dokudovskaya,S., Bordonne,R. and Tazi,J. (2002) A conserved *Drosophila* transportin-serine/arginine-rich (SR) protein permits nuclear import of *Drosophila* SR protein splicing factors and their antagonist repressor splicing factor 1. *Mol. Biol. Cell*, **13**, 2436–2447.

Andersen,J.S., Lyon,C.E., Fox,A.H., Leung,A.K.L., Lam,Y.W., Steen,H., Mann,M. and Lamond,A. (2002) Directed proteomic analysis of the human nucleolus. *Curr. Biol.*, **12**, 1–11.

Blanchette,M. and Chabot,B. (1999) Modulation of exon skipping by high-affinity hnRNP A1-binding sites and by intron elements that repress splice site utilization. *EMBO J.*, **18**, 1939–1952.

Caceres,J.F., Stamm,S., Helfman,D.M. and Krainer,A.R. (1994) Regulation of alternative splicing *in vivo* by overexpression of antagonistic splicing factors. *Science*, **265**, 1706–1709.

Caceres,J.F., Misteli,T., Creaton,G.R., Spector,D.L. and Krainer,A.R. (1997) Role of the modular domains of SR proteins in subnuclear localization and alternative splicing specificity. *J. Cell Biol.*, **138**, 225–238.

Cazalla,D., Zhu,J., Manche,L., Huber,E., Krainer,A.R. and Caceres,J.F. (2002) Nuclear export and retention signals in the RS domain of SR proteins. *Mol. Cell. Biol.*, **22**, 6871–6882.

Eilbracht,J. and Schmidt-Zachmann,M.S. (2001) Identification of a sequence element directing a protein to nuclear speckles. *Proc. Natl Acad. Sci. USA*., **98**, 3849–3854.

Eperon,I.C., Makarova,O.V., Mayeda,A., Munroe,S.H., Caceres,J.F., Hayward,D.G. and Krainer,A,R. (2000) Selection of alternative 5′ splice sites: role of U1 snRNP and models for the antagonistic effects of SF2/ASF and hnRNP A1. *Mol. Cell. Biol.*, **20**, 8303–8318.

Graveley,B.R. (2000) Sorting out the complexity of SR protein functions. *RNA*, **6**, 1197–1211.

Hedley,M.L., Amrein,H. and Maniatis,T. (1995) An amino acid sequence motif sufficient for subnuclear localization of an arginine/serine-rich splicing factor. *Proc. Natl Acad. Sci. USA*, **92**, 11524–11528.

Huber,J., Cronshagen,U., Kadokura,M., Marshallsay,C., Wada,T., Sekine,M. and Luhrmann,R. (1998) Snurportin1, an m3G-cap-specific nuclear import receptor with a novel domain structure. *EMBO J.*, **17**, 4114–4126.

Jackson,F.R., Banfi,S., Guffanti,A. and Rossi,E. (1997) A novel zinc finger-containing RNA-binding protein conserved from fruitflies to humans. *Genomics*, **41**, 444–452.

Jakel,S. and Gorlich D. (1998) Importin β, transportin, RanBP5 and RanBP7 mediate nuclear import of ribosomal proteins in mammalian cells. *EMBO J.*, **17**, 4491–4502.

Jakel,S., Albig,W., Kutay,U., Bischoff,F.R., Schwamborn,K., Doenecke,D. and Gorlich,D. (1999) The importin β/importin 7 heterodimer is a functional nuclear import receptor for histone H1. *EMBO J.*, **18**, 2411–2423.

Jullien,D., Gorlich,D., Laemmli,U.K. and Adachi,Y. (1999) Nuclear import of RPA in *Xenopus* egg extracts requires a novel protein XRIPα but not importin α. *EMBO J.*, **18**, 4348–4358.

Kataoka,N., Bachorik,J.L. and Dreyfuss,G. (1999) Transportin-SR, a nuclear import receptor for SR proteins. *J. Cell Biol.*, **145**, 1145–1152.

Klebe,C., Bischoff,F.R., Ponstingl,H. and Wittinghofer,A. (1995) Interaction of the nuclear GTP-binding protein Ran with its regulatory proteins RCC1 and RanGAP1. *Biochemistry*, **34**, 639–647.

Krecic,A.M. and Swanson,M.S. (1999) hnRNP complexes: composition, structure, and function. *Curr. Opin. Cell Biol.*, **11**, 363–371.

Lai,M.C., Teh,B.H. and Tarn,W.Y. (1999) A human papillomavirus E2 transcriptional activator. The interactions with cellular splicing factors and potential function in pre-mRNA processing. *J. Biol. Chem.*, **274**, 11832–11841.

Lai,M.C., Lin,R.I., Huang,S.Y., Tsai,C.W. and Tarn,W.Y. (2000) A human importin-β family protein, transportin-SR2, interacts with the phosphorylated RS domain of SR proteins. *J. Biol. Chem.*, **275**, 7950–7957.

Lai,M.C., Lin,R.I. and Tarn,W.Y. (2001) Transportin-SR2 mediates nuclear import of phosphorylated SR proteins. *Proc. Natl Acad. Sci. USA*, **98**, 10154–10159.

Leung,A.K. and Lamond,A.I. (2002) *In vivo* analysis of NHPX reveals a novel nucleolar localization pathway involving a transient accumulation in splicing speckles. *J. Cell Biol.*, **157**, 615–629.

Manley,J.L. and Tacke,R. (1996) SR proteins and splicing control. *Genes Dev.*, **10**, 1569–1579.

Mattaj,I.W. and Englmeier,L. (1998) Nucleocytoplasmic transport: the soluble phase. *Annu. Rev. Biochem.*, **67**, 265–306.

Mayeda,A. and Krainer,A.R. (1999) Mammalian *in vitro* splicing assays. *Methods Mol. Biol.*, **118**, 315–321.

McNeil,G.P., Zhang,X., Genova,G. and Jackson,F.R. (1998) A molecular rhythm mediating circadian clock output in *Drosophila*. *Neuron*, **20**, 297–303.

Michael,W.M. (2000) Nucleocytoplasmic shuttling signals: two for the price of one. *Trends Cell Biol.*, **10**, 46–50.

Michael,W.M., Choi,M. and Dreyfuss,G. (1995) A nuclear export signal in hnRNP A1: a signal-mediated, temperature-dependent nuclear protein export pathway. *Cell*, **83**, 415–422.

Mintz,P.J. and Spector,D.L. (2000) Compartmentalization of RNA processing factors within nuclear speckles. *J. Struct. Biol.*, **129**, 241–251.

Nakielny,S. and Dreyfuss,G. (1999) Transport of proteins and RNAs in and out of the nucleus. *Cell*, **99**, 677–690.

Newby,L.M. and Jackson,F.R. (1996) Regulation of a specific circadian clock output pathway by lark, a putative RNA-binding protein with repressor activity. *J. Neurobiol.*, **31**, 117–128.

Ribbeck,K. and Gorlich,D. (2002) The permeability barrier of nuclear pore complexes appears to operate via hydrophobic exclusion. *EMBO J.*, **21**, 2664–2671.

Shopland,L.S. and Lawrence,J.B. (2000) Seeking common ground in nuclear complexity. *J. Cell Biol.*, **150**, F1–F4.

Siomi,M.C., Eder,P.S., Kataoka,N., Wan,L., Liu,Q. and Dreyfuss,G. (1997) Transportin-mediated nuclear import of heterogeneous nuclear RNP proteins. *J. Cell Biol.*, **138**, 1181–1192.

Sleeman,J.E. and Lamond,A.I. (1999a) Nuclear organization of pre-mRNA splicing factors. *Curr. Opin. Cell Biol.*, **11**, 372–377.

Sleeman,J.E. and Lamond,A.I. (1999b) Newly assembled snRNPs associate with coiled bodies before speckles, suggesting a nuclear snRNP maturation pathway. *Curr. Biol.*, **9**, 1065–1074.

Sleeman,J.E., Ajuh,P. and Lamond,A.I. (2001) snRNP protein expression enhances the formation of Cajal bodies containing p80-coilin and SMN. *J. Cell Sci.*, **114**, 4407–4419.

Smith,C.W. and Valcarcel,J. (2000) Alternative pre-mRNA splicing: the logic of combinatorial control. *Trends Biochem. Sci.*, **25**, 381–388.

Tarn,W.Y. and Steitz,J.A. (1994) SR proteins can compensate for the loss of U1 snRNP functions *in vitro*. *Genes Dev.*, **8**, 2704–2717.

van der Houven van Oordt,W., Diaz-Meco,M.T., Lozano,J., Krainer, A.R., Moscat,J. and Caceres,J.F. (2000) The MKK(3/6)-p38-signaling cascade alters the subcellular distribution of hnRNP A1 and modulates alternative splicing regulation. *J. Cell Biol.*, **149**, 307–316.

Yeakley,J.M., Tronchere,H., Olesen,J., Dyck,J.A., Wang,H.Y. and Fu,X.D. (1999) Phosphorylation regulates *in vivo* interaction and molecular targeting of serine/arginine-rich pre-mRNA splicing factors. *J. Cell Biol.*, **145**, 447–455.

Zahler,A.M., Lane,W.S., Stolk,J.A. and Roth,M.B. (1992) SR proteins: a conserved family of pre-mRNA splicing factors. *Genes Dev.*, **6**, 837–847.

Received September 12, 2002; revised January 15, 2003; accepted January 20, 2003